J Appl Electrochem (2008) 38:1143–1149
DOI 10.1007/s10800-008-9551-1

ORIGINAL PAPER

NH_3 decomposition in a proton conducting solid electrolyte cell

**S. Zisekas · G. Karagiannakis · C. Kokkofitis ·
M. Stoukides**

Received: 11 October 2007 / Revised: 7 March 2008 / Accepted: 10 March 2008 / Published online: 19 March 2008

Abstract The reaction of NH_3 decomposition was studied on Ag in a proton conducting double chamber cell-reactor. The proton conductor was a strontia-ceria-ytterbia (SCY) perovskite of the form $SrCe_{0.95}Yb_{0.05}O_{3-\alpha}$. The reaction was studied at 350–700 °C and atmospheric total pressure. The proton transference number (PTN) was calculated by simultaneous measurement of the imposed current and the proton flux and it was found to vary between 0.5 and 0.7. The effects of imposed current, temperature and inlet gas composition on the reaction rate and the PTN, were examined. Although the faradaic efficiency (Λ) remained near unity in all experiments, reaction rate enhancements (ρ) as high as 57 were achieved. An up to 90% decrease in the activation energy of the reaction was observed when protons were electrochemically "pumped" away from the catalyst.

Keywords NH_3 decomposition · Proton conductor · Silver electrode

1 Introduction

Because of the importance of ammonia synthesis, the reverse reaction of ammonia decomposition has been studied extensively on several metals but mainly on the industrial catalysts, Fe and Ru [1–3]. Recently, the reaction has attracted considerable attention as ammonia is a candidate fuel for storing hydrogen for fuel cell applications. Ammonia contains no carbon and thus, the produced hydrogen is CO_x free. This is of major importance for low temperature fuel cells such as the Proton Exchange Membrane Fuel Cell (PEMFC) and the Alkaline Fuel Cell (AFC). For such applications, ammonia is considered to be a better fuel than methanol [4]. Furthermore, ammonia can store more hydrogen than methanol on a mass basis (17.5% vs. 12.5%). Also, theoretical studies have shown that a fuel cell fueled with H_2 produced from NH_3 decomposition constitutes an economically feasible process if hydrogen storage and transportation are taken into account [5].

Moreover, ammonia can be used directly as a fuel in Solid Oxide Fuel Cells (SOFCs) utilizing either O^{2-} [6] or H^+ conductors [7, 8]. Compared to the O^{2-}, the H^+ conducting SOFC seems to be advantageous because ammonia cannot be oxidized to produce NO_x and thus, the only by-products of the fuel cell are water and nitrogen.

In the present work the reaction of ammonia decomposition was studied on Ag electrodes in a proton conducting double-chamber reactor cell. Additionally, the proton transport numbers (PTN) were measured under the employed conditions.

2 Experimental

The reaction was studied in a double-chamber cell-reactor as illustrated in Fig. 1. A strontia-ceria-ytterbia (SCY) perovskite disk of the form $SrCe_{0.95}Yb_{0.05}O_{3-\alpha}$ was used as a proton conductor. The disk thickness was about 1.3 mm and its diameter was 24 mm. The disk was supplied by CERECO (Greece) and was prepared according to the

---

S. Zisekas · G. Karagiannakis · C. Kokkofitis · M. Stoukides
Chemical Engineering Department, Aristotle University,
University Box 1517, Thessaloniki 54124, Greece

S. Zisekas · G. Karagiannakis · C. Kokkofitis ·
M. Stoukides (✉)
Chemical Process Engineering Research Institute,
University Box 1517, Thessaloniki 54124, Greece
e-mail: stoukidi@cperi.certh.gr

procedure followed by Iwahara et al. [9]. The disk was sealed at the bottom end of a 150 mm long yttria stabilized zirconia (YSZ) tube (16 mm ID, 19 mm OD), using a BaO–SiO_2 glass sealing. The YSZ tube with the disk were enclosed in a 20 cm long quartz tube (38 mm ID, 42 mm OD), closed at its bottom end.

On the two sides of the SCY disk, two porous Ag electrodes were deposited. The working electrode was deposited on the inside surface of the disk (Fig. 1) and had a superficial surface area of approximately 2 cm^2. The counter electrode was deposited on the outside surface of the disk and had a superficial surface area of approximately 5 cm^2. Both electrodes were prepared by painting the SCY surface with a silver conductive ink (Alfa Aesar, #41823), followed by calcination in air, for 1 h at 500 °C and then, for 2 h at 750 °C. The catalyst loading for the working electrode was 16 mg. Scanning Electron Micrographs showed that the average diameter of the Ag crystallites was about 0.5 μm. Using this average size and the mass of the catalyst, a catalytic surface area of 180 cm^2 was calculated.

Ammonia diluted in helium (99.999% purity) was fed to the inner chamber of the reactor i.e. inside the YSZ tube, while argon was flowing in the outer chamber. The volumetric flowrate of the reaction mixture varied from 10 to 20 mL STP min^{-1}, while that of argon from 5 to 20 mL STP min^{-1}. Analysis of the inlet and outlet gaseous stream of either chamber was performed by on-line gas chromatography using a HP 5890 series II gas chromatograph with a thermal conductivity detector, equipped with a Molecular Sieve 5A and a Hayesep Q columns. Currents and voltages across the cell were imposed using a 2053 AMEL Galvanostat-Potentiostat.

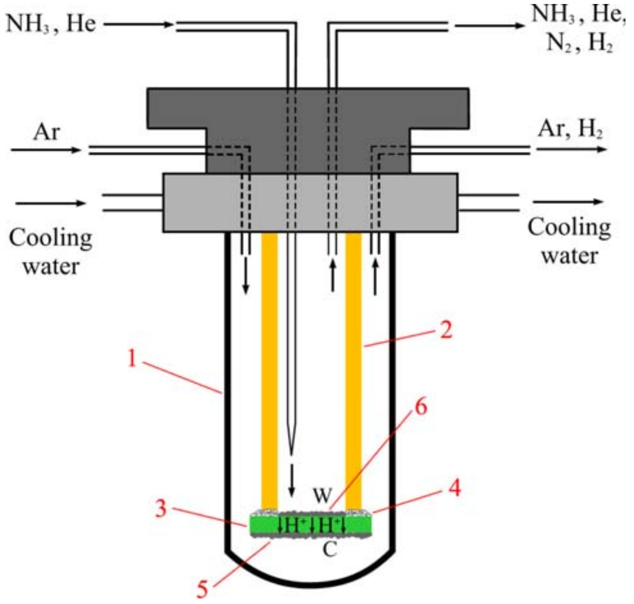

Fig. 1 Schematic diagram of the H^+ conducting double-chamber cell-reactor (1): Quartz tube, (2): YSZ tube, (3): Proton conductor (SCY) (4): Glass sealing, (5): Counter electrode, (6): Working electrode

One of the applications of H^+ conductors is their use as ionic (protonic) pumps. For a pure H^+ conductor, the molar flux of hydrogen through the cell is calculated according to Faraday's law and is equal to I/2F moles of H_2 s^{-1}, where I is the imposed current. For a mixed conductor the PTN has to be measured in order to calculate the hydrogen flux.

The change in the rate of hydrogen production at the cathode can be compared to I/2F, the rate of electrochemical transport of hydrogen through the solid electrolyte. To this end, two dimensionless factors, Λ and ρ, have been introduced by Vayenas et al. [10, 11]:

$$\Lambda = \frac{\Delta r}{\frac{I}{2\cdot F}} \tag{1}$$

and

$$\rho = \frac{r}{r_o} \tag{2}$$

where r, r_o are the electrocatalytic (closed circuit) and catalytic (open circuit) reaction rates and Δr is the induced change in the catalytic rate of hydrogen production or consumption (in moles per second). When Δr is equal to the rate of H^+ transport through the solid electrolyte, the cell operation is Faradaic, i.e. $\Lambda = 1$. It has been observed in several cases, however, that Λ can exceed unity. This is the case of Non-Faradaic Electrochemical Modification of Catalytic Activity (NEMCA effect). This effect has been attributed to changes in the catalyst work function caused by ionic pumping [10, 11].

If a mixed conductor is used, Eq. 1 is modified as:

$$\Lambda = \frac{\Delta r}{\frac{I_t}{2\cdot F}\cdot \mathrm{PTN}} \tag{3}$$

where I_t is the measured electrical current.

3 Results

The decomposition of NH_3 was studied at 350–700 °C and at atmospheric total pressure under both open and closed circuit conditions. Ammonia–helium mixtures were fed in the reactor and in order to avoid mass transport effects, the partial pressure of ammonia, P_{NH_3}, was kept below 2 kPa. In the closed circuit experiments, the reaction was studied galvanostatically, i.e. upon imposing constant positive or negative currents through the cell. Arbitrarily, a current was considered positive when protons were "pumped" away from the working electrode (inside surface of the SCY disk, Fig. 1).

For SCY, the PTN values reported in the literature vary considerably [12–15]. Thus, separate measurements had to be performed in order to measure the electrochemical hydrogen flux under the employed conditions. In order to do that, the exit stream from the outer chamber was connected to the GC. It was then possible to measure the concentration of H_2 (and consequently calculate the hydrogen flux) in the outer chamber. The PTN was calculated by dividing the measured flux by $I_t/2 \cdot F$. Figure 2 shows the dependence of PTN on current density (measured current density) at various temperatures between 500 and 700 °C and for $P_{NH_3} = 2$ kPa. It can be seen that at 500–600 °C the PTN varies from 0.6 to 0.7. At temperatures between 350 and 450 °C (not shown in Fig. 2), PTN increased with current density from 0.3 to 0.6.

At 650 and 700 °C the curves exhibit a maximum at about 1–1.5 mA cm^{-2}; at higher currents, PTN decreases rapidly. This decrease in PTN was accompanied by the production of NO at the anode. The production of NO was attributed to the reaction of NH_3 with the perovskite oxide rather than with gaseous O_2 (inevitably there was an oxygen leak in the anode chamber), because the concentration of O_2 was very low, less than 100 ppm. In a separate set of experiments, it was found that the long term operation under such conditions decreased significantly the cell performance and finally resulted in its complete deterioration.

Figure 3 shows the effect of P_{NH_3} on PTN at 600 °C. At current densities up to 2 mA cm^{-2}, there is a positive effect on PTN, while at higher current densities the PTN decreases. This negative effect is more pronounced at lower P_{NH_3}.

Figure 4 shows the open circuit catalytic rates obtained for $P_{NH_3} = 2$ kPa at various temperatures. At temperatures below 500 °C, the reaction rate was negligible and thus, the data are not presented in the figure. Also, "blank" experiments performed in the absence of the Ag electrode showed that the YSZ tube is inactive for this reaction at temperatures below 650 °C.

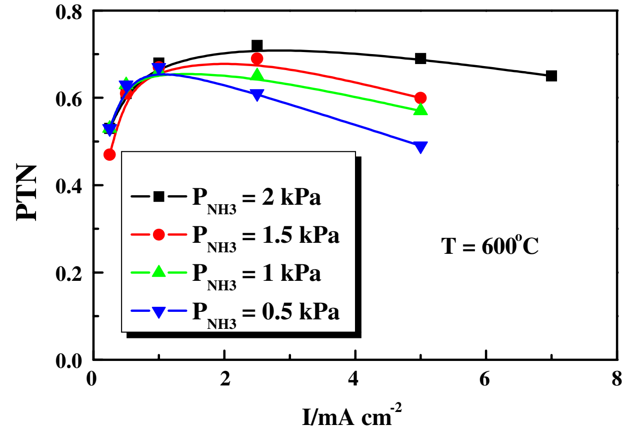

Fig. 3 Dependence of proton transference number (PTN) on current density (I) at various ammonia partial pressures. T = 600 °C

Figure 5a, b and c, illustrate the dependence of the reaction rate on the electrochemical hydrogen flux, at temperatures between 350 and 700 °C and at $P_{NH_3} = 2$ kPa. It should be pointed out that the value of I/2F is the "true" hydrogen flux through the solid electrolyte, i.e. $I = I_t \times$ PTN. In all cases the reaction rate increases significantly with current. It can also be seen (Fig. 5a and b) that at temperatures below 500 °C, the open-circuit (catalytic) rate was negligible.

The effect of P_{NH_3} is presented in Fig. 6. The reaction rate is plotted versus I/2F at 600 °C. The reaction rate increases with current in all cases. From the data of this figure, Fig. 7 can be constructed, where the logarithm of r_{NH_3} is plotted versus the logarithm of P_{NH_3}. According to Tamaru [16], at high temperatures and low hydrogen

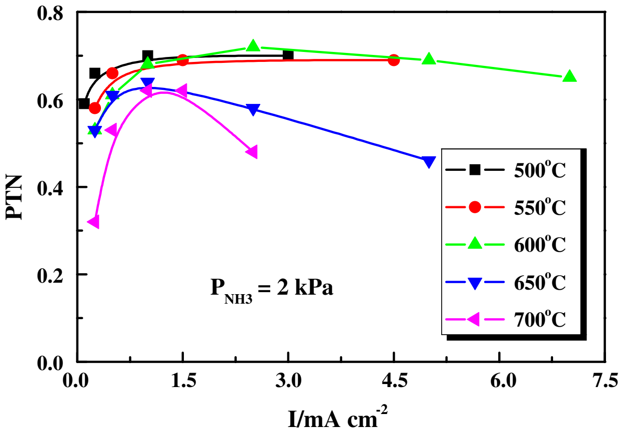

Fig. 2 Dependence of proton transference number (PTN) on current density (I) at various temperatures. $P_{NH_3} = 2$ kPa

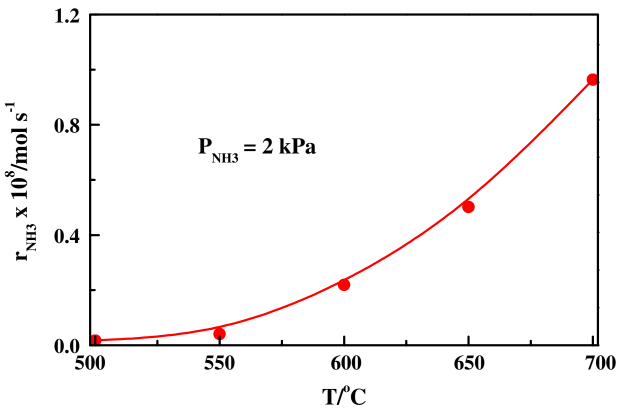

Fig. 4 Temperature dependence of the open-circuit rate of NH_3 decomposition. $P_{NH_3} = 2$ kPa

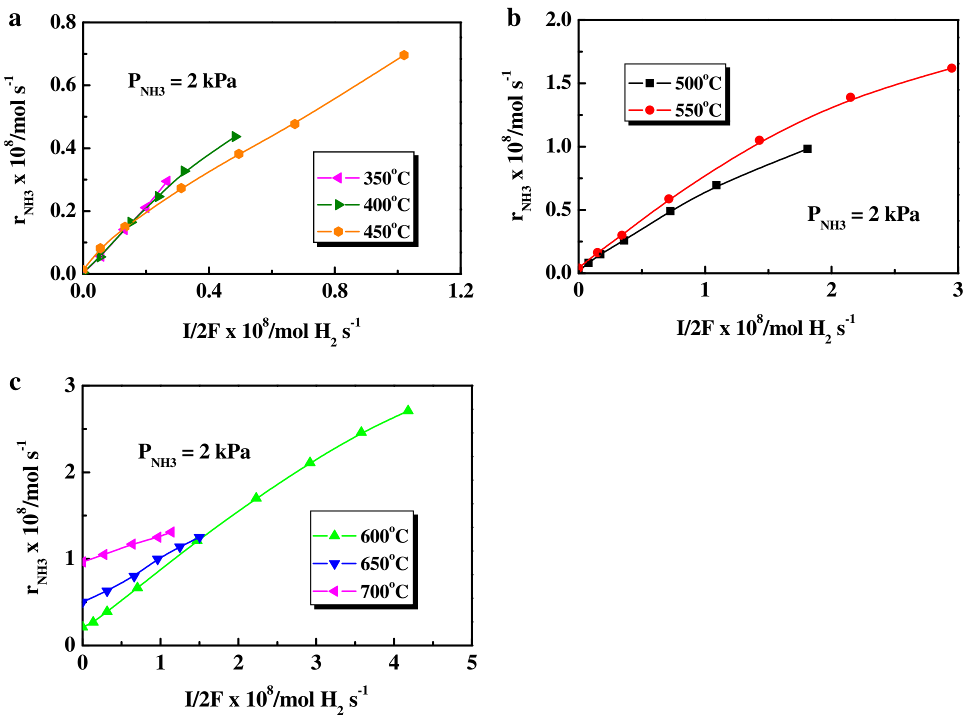

Fig. 5 (**a**) Dependence of reaction rate on rate of proton removal from the catalyst surface. P_{NH_3} = 2 kPa, T = 350, 400 and 450 °C. (**b**) Dependence of reaction rate on rate of proton removal from the catalyst surface. P_{NH_3} = 2 kPa, T = 500 and 550 °C. (**c**) Dependence of reaction rate on rate of proton removal from the catalyst surface. P_{NH_3} = 2 kPa, T = 600, 650 and 700 °C

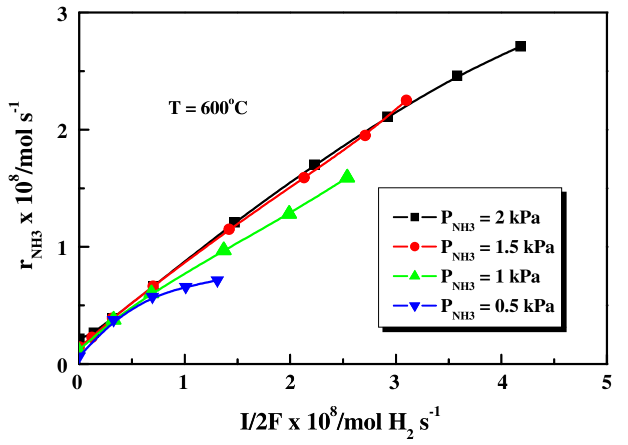

Fig. 6 Dependence of reaction rate on rate of proton removal from the catalyst surface at various ammonia partial pressures. T = 600 °C

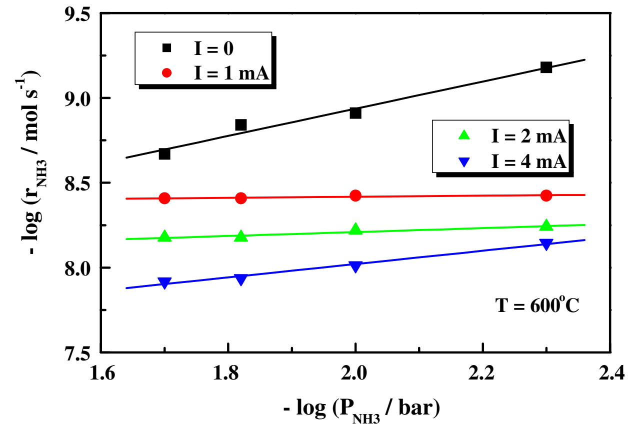

Fig. 7 Logarithmic dependence of reaction rate on P_{NH_3} at various currents. T = 600 °C

partial pressures, the ammonia decomposition follows power law kinetics:

$$r_{NH_3} = k \cdot P_{NH_3}{}^{q_{app}} \tag{4}$$

where q_{app} is the apparent reaction order. Thus, from the linear fit of the data of Fig. 7, q_{app} can be calculated. The results presented in Table 1 show that the highest q_{app} is that obtained under open circuit. Furthermore, the lower the value of the current the greater the deviation from the open circuit value.

The dependence of the faradaic efficiency, Λ, and the corresponding rate enhancement ratio, ρ, on I/2F, is presented in Fig. 8. Upon "pumping" protons away from the working electrode (catalyst), ρ increases while Λ decreases. This behaviour was observed at all temperatures examined. Although the maximum value of ρ is 57, i.e. there is an up to 5600% increase in the catalytic rate, Λ hardly exceeds unity.

Table 1 The apparent reaction order (q_{app}) calculated at 600 °C under both, open and closed circuit conditions

I (mA)	0	1	2	4
q_{app}	0.8 ± 0.1	0.03 ± 0.01	0.12 ± 0.02	0.39 ± 0.03

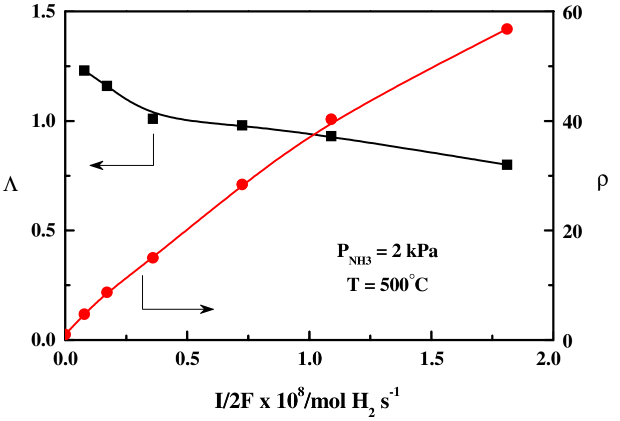

Fig. 8 Dependence of faradaic efficiency (Λ) and reaction rate enhancement (ρ) on rate of proton removal from the catalyst surface. P_{NH_3} = 2 kPa, T = 500 °C

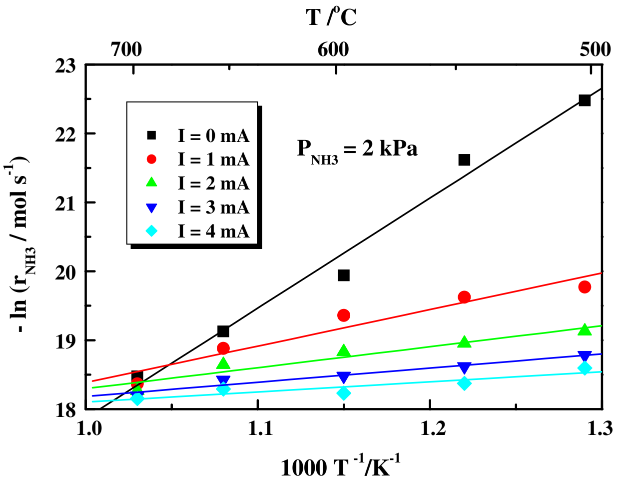

Fig. 10 Logarithmic dependence of reaction rate on reciprocal temperature at various currents. P_{NH_3} = 2 kPa

Table 2 The apparent activation energy calculated under both open and closed circuit conditions with the ammonia partial pressure kept at 2 kPa

I (mA)	0	1	2	3	4
E_{act} (kJ mol^{-1})	133 ± 10	44 ± 7	25 ± 4	17 ± 2	12 ± 3

The effect of temperature on Λ and ρ at constant current and P_{NH_3} is shown in Fig. 9a and b, respectively. Figure 9a shows that Λ decreases with temperature and thus, at T > 550 °C, the cell operation becomes subfaradaic ($\Lambda < 1$). Figure 9b shows a significant decrease in ρ with temperature, a behavior which is expected because the open-circuit rate, r_o, increases with temperature (Eq. 2). The value of ρ corresponding to 500 °C is not possible to be presented, as it tends to infinite due to the negligible open circuit rate ($r_o \cong 0$).

The open circuit data as well as the data presented in Fig. 9a and b, can be used for the construction of the Arrhenius plots of Fig. 10. From the slopes of the lines, the apparent activation energy, $E_{act,}$ can be calculated and results are presented in Table 2. A considerable decrease in E_{act} is induced upon imposing a current through the cell and the higher the current the lower the value of E_{act}. At the highest current (4 mA), the value of E_{act} is more than an order of magnitude lower than its open circuit value.

In all the above presented closed-circuit experiments (Figs. 5–9), only positive currents were imposed, i.e. protons were “pumped” away from the catalyst. It was found that upon imposing negative currents, i.e. electrochemically supplying protons to the catalyst, there was no measurable effect on the reaction rate.

4 Discussion

Although numerous works on the catalytic decomposition of NH_3 can be found in the literature, only a few studies conducted in solid electrolyte cells have been reported [17–20]. Pitselis et al. [17] studied the reaction using Fe as the working electrode and $CaZr_{0.9}In_{0.1}O_{3-\alpha}$ as the proton conductor, at temperatures between 530 and 600 °C. The electrophobicity of the reaction was accompanied by a strong non-faradaic effect with a maximum rate enhancement factor Λ equal to 120. Nevertheless, due to the higher

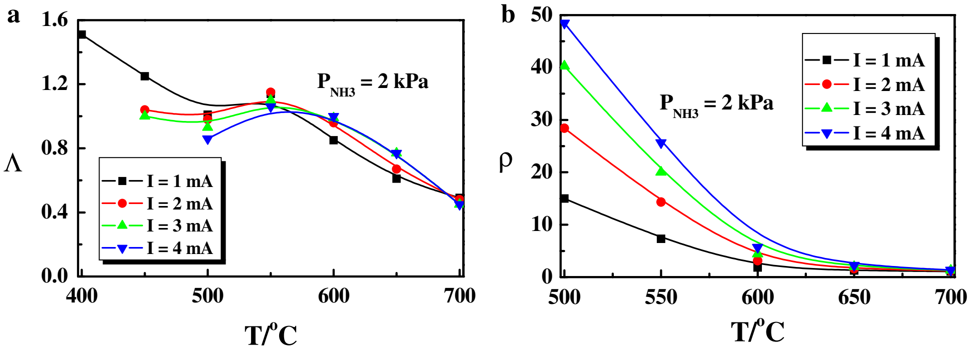

Fig. 9 (**a**) Dependence of faradaic efficiency (Λ) on temperature at various currents. P_{NH_3} = 2 kPa. (**b**) Dependence of reaction rate enhancement (ρ) on temperature at various currents. P_{NH_3} = 2 kPa

open circuit rates and the low imposed currents the maximum increase with respect to the catalytic rate was 3.6 (i.e. $\rho = 3.6$). Skodra et al. [19] studied the reaction in a SCY single chamber reactor cell using Ru and Ag electrodes. They found that the reaction rate was increasing by both positive and negative currents. Positive currents corresponded to proton pumping from Ru, while negative from Ag. It was found that when Ru was used as the working electrode i.e. on positive currents, the current effect was more profound. The maximum Λ value obtained was about 4. Marnellos and Stoukides [18] studied the reaction on Pd in a SCY double-chamber cell. At 570 °C and upon imposing negative currents ("pumping" protons to the catalyst), an almost linear decrease of the reaction rate with I/2F, was observed.

In a previous work in our Laboratory [20], the reaction was studied in a single-chamber cell-reactor on Ag electrodes. Hence, the data obtained therein can be combined with the present double-chamber results for a safer interpretation and understanding of the reaction mechanism.

Silver is not an active catalyst for the catalytic decomposition of NH_3. The reaction exhibits an apparent activation energy of 133 ± 10 kJ mol^{-1} between 500 and 700 °C. This value is in agreement with our previous work, in which it was found equal to 115 ± 4 kJ mol^{-1} between 550 and 650 °C [20]. Also in good agreement are the values of the apparent reaction order calculated here and in [20], i.e. 0.8 ± 0.1 vs. 0.88 ± 0.1. Furthermore, there is agreement with previous studies on various catalysts reporting that at low temperatures the reaction is zero order in NH_3 and becomes first order at higher temperatures [1, 21–24].

Although Ag exhibits relatively low activity for the decomposition of NH_3 the closed-circuit results have shown that the reaction rate increases significantly by "pumping" protons away from the catalyst. The increase in reaction rate with increasing the catalyst potential ($\Delta V_{WR} > 0$) implies that the reaction exhibits an electrophobic behavior. The maximum increase of 5600% ($\rho = 57$) was observed at 500 °C. It is worth mentioning that these high ρ values correspond to very low Λ's ($\Lambda < 2$). Low Λ's were also observed in the single-chamber study [20]. In the latter, the ρ's were quite lower than those reported here ($\rho < 3.4$). This should be expected because (a) the catalyst loading in [20] was about 8 times higher than now and (b) in the single chamber both electrodes contribute to the open circuit rate as they are both exposed to the reacting mixture.

The low Λ values obtained can be explained by the following equation:

$$|\Lambda| \simeq \frac{2 \cdot F \cdot r_o}{I_o} \tag{5}$$

where I_o is exchange current at the electrode-electrolyte interface. This equation has been used successfully in order to calculate the magnitude of $|\Lambda|$ in a large number of catalytic systems [10, 11]. According to this equation, Λ is proportional to the open circuit reaction rate and inversely proportional to the exchange current. Values of I_o at the Ag-SCY interface have been reported in the literature [25] for various hydrogen contents of the gas phase. At temperatures and gas compositions similar to the present work, I_o attains values of the order of 10^{-3} A cm^{-2}. The open circuit reaction rates, r_o, on the other hand, are of the order of 10^{-8} moles s^{-1} cm^{-2} (Figs. 4–6). With the above I_o and r_o values introduced in Eq. 5, Λs of the order of unity are predicted. Thus, the validity of Eq. 5 is verified (Figs. 8 and 9a).

The decrease in the apparent reaction order upon imposing a positive current, can be attributed to the electron donor character of ammonia adsorbed on metal surfaces [26, 27]. Specifically, the increase in the catalyst work function upon imposing a positive current corresponds to an increase in ammonia coverage on catalyst surface. Thus, a weaker dependence on ammonia partial pressure is expected. The observation that initial pronounced decrease in reaction order is followed by a gradual increase with increasing current can be explained if the conversion of ammonia at various P_{NH_3} is considered. Table 3 shows the ρ values obtained at various P_{NH_3}. For the same current, ρ is higher at low P_{NH_3}. But because NH_3 is the reactant, inevitably a very high increase in ρ, will gradually make stronger the dependence on P_{NH_3}.

The 90% decrease in the apparent activation energy observed upon "pumping" protons away from the catalyst is impressive. This phenomenon has been observed in several electrochemical promotion studies [10]. For the reaction under study, Skodra et al. [19] observed a similar decrease, while Pitselis et al. [17] observed the opposite, i.e. an increase in the activation energy. It is well established [10, 11] that in a wide temperature range, the catalyst work function can be calculated from the following equation:

$$\Delta(e\Phi) = e \cdot \Delta V_{WR} \tag{6}$$

Table 3 The values of rate enhancement ratio corresponding to the data of Fig. 7

P_{NH_3} (kPa)	2	1.5	1	0.5
I (mA)	ρ			
1	1.8	2.7	3.1	5.7
2	3.1	4.6	4.9	8.7
4	5.7	7.9	7.9	10.9

The above equation shows that a change in cell potential corresponds to an analogous change of the catalyst work function and consequently, to the chemisorptive bond strength of reactants and intermediates. In the present study, the observed decrease in the activation energy upon "pumping" protons away from the catalyst can be attributed to the weakening of the adsorption strength of atomically adsorbed nitrogen. Thus, the recombinative desorption of nitrogen, which is considered the rate determining step [28], is enhanced.

5 Conclusions

The present results show that under the employed conditions SCY is a mixed (protonic–electronic) conductor, with the PTN varying generally between 0.5 and 0.7. High current densities caused a decrease in PTN, an effect that was more pronounced at higher temperatures and lower NH_3 partial pressures.

Although the faradaic efficiencies attained were near unity, a strong increase in the reaction rate was induced upon proton "pumping" from the catalyst surface. The catalytic activity of Ag increased reversibly by as much as 5600% (maximum $\rho = 57$).

Acknowledgement We gratefully acknowledge financial support of this research by the Center for Research and Technology Hellas (CE.R.T.H.) of Thessaloniki.

References

1. Grunze M (1982) In: King DA, Woodruff DP (eds) The chemical physics of solid surfaces and heterogeneous catalysis, vol 4. Elsevier
2. Nielsen A (1981) Cat Rev - Sci Eng 23:17
3. Lambert RM, Bridge ME (1982) In: King DA, Woodruff DP (eds) The chemical physics of solid surfaces and heterogeneous catalysis, vol 3B. Elsevier
4. Metkemeijer R, Achard P (1994) Int J Hydrogen Energy 19:535
5. Metkemeijer R, Achard P (1994) J Power Sources 49:271
6. Wojcik A, Middleton H, Damopoulos I, Herle JV (2003) J Power Sources 118:342
7. McFarlan A, Pelletier L, Maffei N (2004) J Electrochem Soc 151:A930
8. Maffei N, Pelletier L, Charland JP, McFarlan A (2005) J Power Sources 140:264
9. Iwahara H, Esaka T, Uchida H, Maeda N (1981) Solid State Ionics 3/4:79
10. Vayenas CG, Jaksic MM, Bebelis S, Neophytides SG (1996) In: Bockris JO'M, Conway BE, White WRE (eds) Modern aspects in electrochemistry. Plenum, New York
11. Vayenas G, Bebelis S, Pliangos C, Brosda S, Tsiplakides D (2001) Electro-chemical activation of catalysis. Kluwer Academic/Plenum, New York
12. Chiang PH, Eng D, Stoukides M (1993) Solid State Ionics 61:99
13. Bonanos N, Ellis B, Mahmood MN (1988) Solid State Ionics 28–30:579
14. Hamakawa S, Hibino T, Iwahara H (1993) J Electrochem Soc 140:459
15. Hamakawa S, Hibino T, Iwahara H (1994) J Electrochem Soc 141:172
16. Tamaru K (1988) Acc Chem Res 21:88
17. Pitselis GE, Petrolekas PD, Vayenas CG (1997) Ionics 3:110
18. Marnellos G, Stoukides M (1998) Science 282:98
19. Skodra A, Ouzounidou M, Stoukides M (2006) Solid State Ionics 177:2217
20. Zisekas S, Karagiannakis G, Marnellos G, Stoukides M (2002) Ionics 8:118
21. Choudhary TV, Santra AK, Sivadinarayana C, Min BK, Yi CW, Davis K, Goodman DW (2001) Catal Lett 77:1
22. Oyama ST (1992) J Catal 133:358
23. Hashimoto K, Toukai N (2000) J Mol Catal A Chem 161:171
24. Chellappa AS, Fischer CM, Thomson WJ (2002) Appl Catal A Gen 227:231
25. Chiang PH, Eng D, Tsiakaras P, Stoukides M (1995) Solid State Ionics 77:305
26. Fisher GE (1981) Chem Phys Lett 79:452
27. Weiss M, Ertl G, Nitschke F (1979) Appl Surf Sci 0:614
28. Egawa C, Nishida T, Naito S, Tamaru K (1984) J Chem Soc Faraday Trans I80:1595